High-resolution low-cost LCD 3D printing for microfluidics and organ-on-a-chip devices

Houda Shafique[1,2], Vahid Karamzadeh[1,2], Geunyong Kim[1,2], Molly L. Shen[1,2], Yonatan Morocz[1,2], Ahmad Sohrabi-Kashani[1,2], and David Juncker[1,2 *]

1. Biomedical Engineering Department, McGill University, Montreal, Quebec, Canada
2. McGill Genome Centre, McGill University, Montreal, Quebec, Canada

[*] Corresponding Author, Email: david.juncker@mcgill.ca

Supplementary information

Supplementary calculations

Supplementary tables

Supplementary figures

Supplementary videos

Supplementary calculations

Section S1. Measurement of surface roughness

The surface roughness of a 3D printed part was measured using profilometry according to the ISO 4287 and 4288 standards. Sample prints that were 25 × 75 × 2 mm^3 (width × length × height) were assessed for surface roughness. The mean surface roughness is given by the average distance between the mean line and all the data points over a minimum sampling length of 0.8 mm; the surface roughness (R_a) is calculated as follows:

$$R_a = \frac{1}{n}\sum_{i=1}^{n}|y_i| \qquad \text{(Equation S1)}$$

where y denotes all the sampled points, and n denotes the number of sampled points that are iterated over an increment i. Over three unique sampling lengths, the average surface roughness of PLInk on the low-cost 3D printers was 530 ± 110 nm (**Figure S4**).

Section S2. Calculation of mixing index

The mixing efficiency was assessed by measuring the fluorescent intensity of a pre-mixed solution versus a solution mixed in the microchannels. The captured images of the mixed solutions were analyzed in ImageJ by taking the fluorescent intensity readout over the length of the channel outlet. For all the flow rates and the given channel geometry, we calculated the corresponding relative mixing index (RMI) as a metric for efficiency as follows:

$$RMI = \left[1 - \frac{\sigma}{\sigma_0}\right] \times 100\% = \left[1 - \frac{\sqrt{\frac{\sum_{i=1}^{n}\left(x_i - x_{avg}\right)^2}{n}}}{\sqrt{\frac{\sum_{i=1}^{n}\left(x_{0i} - x_{avg}\right)^2}{n}}}\right] \times 100\% \qquad \text{(Equation S2)}$$

where σ and σ_0 are the STDs of the fluorescent intensities, x_i is the normalized intensity at point i at the outlet, x_{0i} is the normalized intensity at point i at the inlet, x_{avg} is the normalized intensity for a completely mixed solution, and n denotes the number of points sampled. With this metric, RMI = 100% represents a state with complete mixing while RMI = 0% represents a state with no mixing.

Section S3. Calculation of the predicted valve closing pressure

Based on known valve dimensions and known material properties, we can estimate the pressure required to deflect the membrane and make contact with the valve seat to subsequently close the valve. For the valve we present here, the predicted valve closing pressure (P) can be calculated as follows:[1]

$$P_{closing} = \left(\frac{5.33}{1-v^2}\left(\frac{y}{t}\right) + \frac{2.6}{1-v^2}\left(\frac{y}{t}\right)^3\right)\left(\frac{Et^4}{r^4}\right) \quad \text{(Equation S3)}$$

where E is the Young's modulus (~68 MPa), v is the Poisson ratio (~0.9), r is the membrane radius (~1.05 mm), t is the membrane thickness (~43 μm), and y is the gap height that the membrane must deflect (~100 μm). This yields a pressure of ~45 kPa to close the valve, which is in good agreement with the physical experiment.

Supplementary tables

Table S1. Summary of 3D printing settings.

	Calibration devices (Figure S5-7)	**Calibration devices** (Figure S8)	**Microfluidic mixer** (Figure 3)	**Membrane microvalve** (Figure 4)	**ELISA-chip** (Figure 5)	**OoC device and 384-well plate** (Figure 6)	**Stacked OoC devices** (Figure 6)
Printer (ELEGOO)	Mars 3 Pro 4K	Mars 4 Ultra 9K	Mars 3 Pro 4K	Saturn 2 8K	Mars 3 Pro 4K	Saturn 3 Ultra 12K	Saturn 3 Ultra 12K
Device dimensions [mm^3]	~26.5 × 4.4 × 3.0	16.9 × 4.6 × 2.0	45.1 × 9.8 × 1.5	42.0 × 42.0 × 2.0	88.7 × 27.3 × 2.8	8.5 × 4.0 × 7.0	8.5 × 4.0 × 7.0
Light engine*	36 COB LED + Fresnel lens	36 COB LED + Fresnel lens	36 COB LED + Fresnel lens	48 COB LED + Fresnel lens	36 COB LED + Fresnel lens	COB LED + refractive lens	COB LED + refractive lens
Light uniformity and angle*	92%	92%, <5°	92%	Not reported	92%	Not reported	Not reported
Pixel size [μm^2]*	35 × 35	18 × 18	35 × 35	28.5 × 28.5	35 × 35	19 × 24	19 × 24
Pixel number [pixels]*	4098 × 2560 ≅ 10M	8520 × 4320 ≅ 36M	4098 × 2560 ≅ 10M	7680 × 4320 ≅ 33M	4098 × 2560 ≅ 10M	11520 × 5120 ≅ 58M	11520 × 5120 ≅ 58M
Build volume [mm^3]*	143 × 89.6 × 175	153.4 × 77.8 × 175	143 × 89.6 × 175	219 × 123 × 250	143 × 89.6 × 175	219 × 123 × 260	219 × 123 × 260
Layer height [mm]	0.020	0.020	0.020	0.020	0.020	0.020	0.050
Exposure time [s]	1.3	1.3	1.6	1.5	1.8	1.5	3.5
Bottom exposure time [s]	7	7	10	10	7	10	10
Rest time [s]	3	3	3	3	5	4	3
Lifting speed [mm min^{-1}]	50	50	30	65	50	65	40
Retract speed [mm min^{-1}]	210	210	60	80	210	210	300
Anti-aliasing	Yes	Yes	Yes	Yes	No	Yes	Yes
Total print time [min]	~51	~51	~39	~31	~42	~86	~486

Chip-on-board LEDs are called COB. * indicates manufacturer information taken from their website at https://www.elegoo.com.

Table S2. Viscosity of 3D printing inks

Ink	**Viscosity [mPa s]***
PLInk containing 0% PETTA crosslinker	16.2
PLInk containing 0.5% PETTA crosslinker	15.8
PLInk containing 1% PETTA crosslinker	15.0
PLInk containing 2% PETTA crosslinker	15.6
Anycubic upgraded ABS-like clear resin	*224*
Monocure 3D crystal clear resin	*551*
Luvantix 3DMaterials clear resin	*528*

* viscosity was measured at 21ºC

Table S3. Summary of Taguchi Design of Experiments assay results

	Capture antibody [µg mL^{-1}]	**Detection antibody [µg mL^{-1}]**	**pHRP [µg mL^{-1}]**	**Relative signal intensity [0-1]**
1	50	1	1	0.42
2	50	5	5	0.59
3	50	25	25	0.63
4	100	1	5	0.55
5	100	5	25	0.63
6	100	25	1	0.51
7	200	1	25	0.61
8	200	5	1	0.59
9	200	25	5	0.67

Table S4. Analysis of variance and percent contribution from Taguchi Design of Experiments

Source	Degree of freedom	Sum of squares	F ratio	p-value	Contribution
pHRP	2	114.3	18.9	0.050	25%
dAb	2	104.5	12.4	0.054	24%
cAb	2	200.0	33.3	0.029*	47%

* for significance level α=0.05

See Luo *et al.*[2] for more details.

Table S5. ELISA-chip cost breakdown using PLInk and assay reagents

Category	**Item**	**Vendor**	**Price [USD]**	**Quantity**	**Cost per chip [USD]**
Ink	PEGDA-250	Sigma-Aldrich	$142	500 mL	$2.15
	ITX	Fisher Scientific	$205	25 g	$0.03
	TPO	Sigma-Aldrich	$159	50 g	$0.01
	PETTA	Sigma-Aldrich	$110	250 mL	$0.04
Assembly	Nitrocellulose	Pall Corporation	$40	25 mm × 3 m	$0.02
	Cover layer	3M	$320	152 mm × 23 m	$0.24
	Absorbent pad	Ahlstrom-Munksjö	$85	200 × 200 mm^2	$0.02
Assay	Mouse anti-human IFN-γ capture antibody	R&D Systems	$489	200 µL at 500 µg mL^{-1}	$0.34
	Biotinylated mouse anti-human IFN-γ detection antibody	R&D Systems	$701	250 µL at 200 µg mL^{-1}	$0.63
	Streptavidin-pHRP	ThermoFisher Scientific	$400	500 µL at 500 µg mL^{-1}	$0.36
	DAB substrate	Sigma-Aldrich	$213	50 tablets at 5 mL per reaction	$0.04
	BSA-biotin	Sigma-Aldrich	$147	1 mL at 10 mg mL^{-1}	$0.01
				Total	$3.89

Table S6. OoC device cost breakdown using PLInk

Item	Vendor	Price [USD]	Quantity	Cost per chip [USD]	
				Individual OoC device (8.9 × 4.5 × 7 mm^3 ≅ 0.17 mL)*	**384-well plate OoC (128 × 85 × 7.5 mm^3 ≅ 50 mL)***
PEGDA-250	Sigma-Aldrich	$142	500 mL	$0.07	$21.50
ITX	Fisher Scientific	$205	25 g	$0.01	$0.30
TPO	Sigma-Aldrich	$159	50 g	$0.01	$0.10
PETTA	Sigma-Aldrich	$110	250 mL	$0.01	$0.40
			Total	$0.10	$22.30

* indicates the volume of the printed block minus the volume of the voids

Supplementary figures

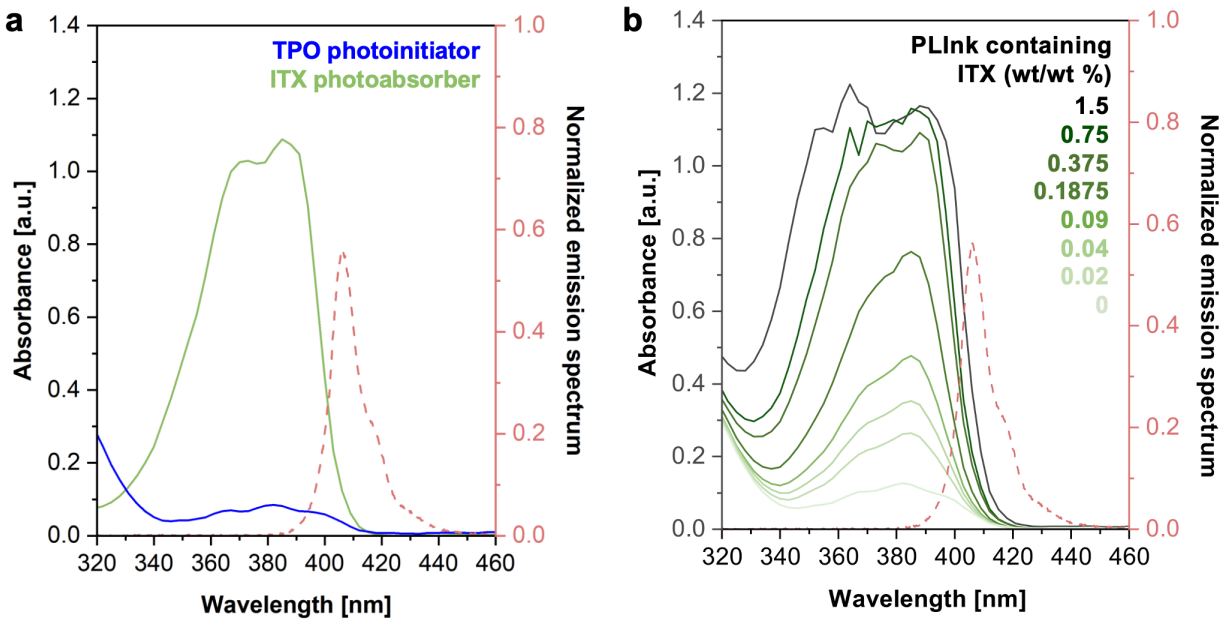

Figure S1. UV-Vis spectra. (a) UV-Vis spectrum of TPO photoinitiator and ITX photoabsorber dissolved in PEGDA-250 (left y-axis) compared to the LCD 3D printer emission spectrum (red dashed line, right y-axis). (b) PLInk UV-Vis spectra formulated with a varying concentration of ITX from 0-1.5% wt/wt showing that higher ITX concentration increased the absorbance at the illumination wavelength of 3D printer (i.e., ~405 nm).

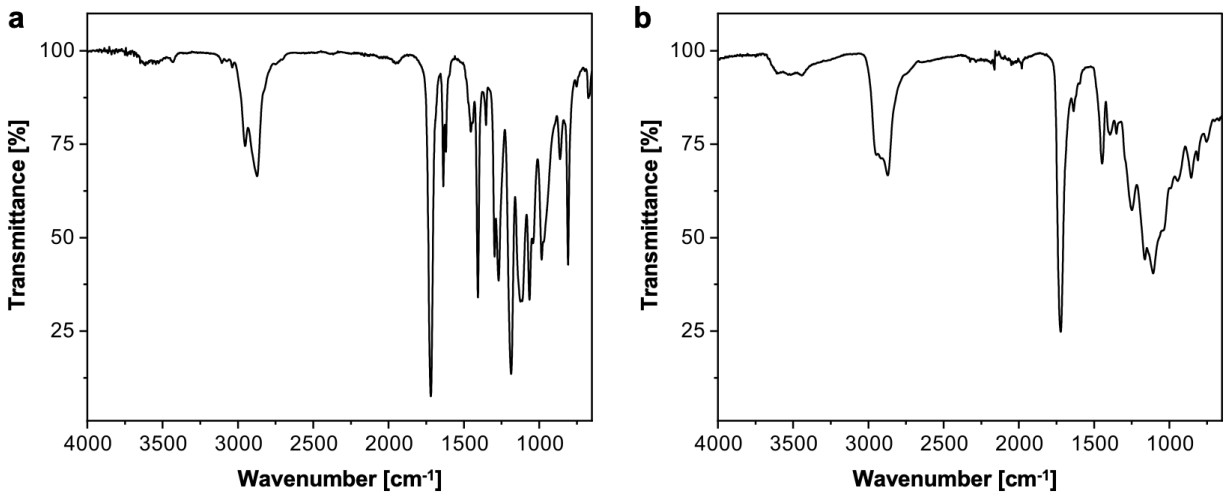

Figure S2. FTIR-ATR spectra. Functional group characterization using FTIR-ATR of the (a) uncured precursor PLInk and (b) cured PLInk following 405 nm UV exposure.

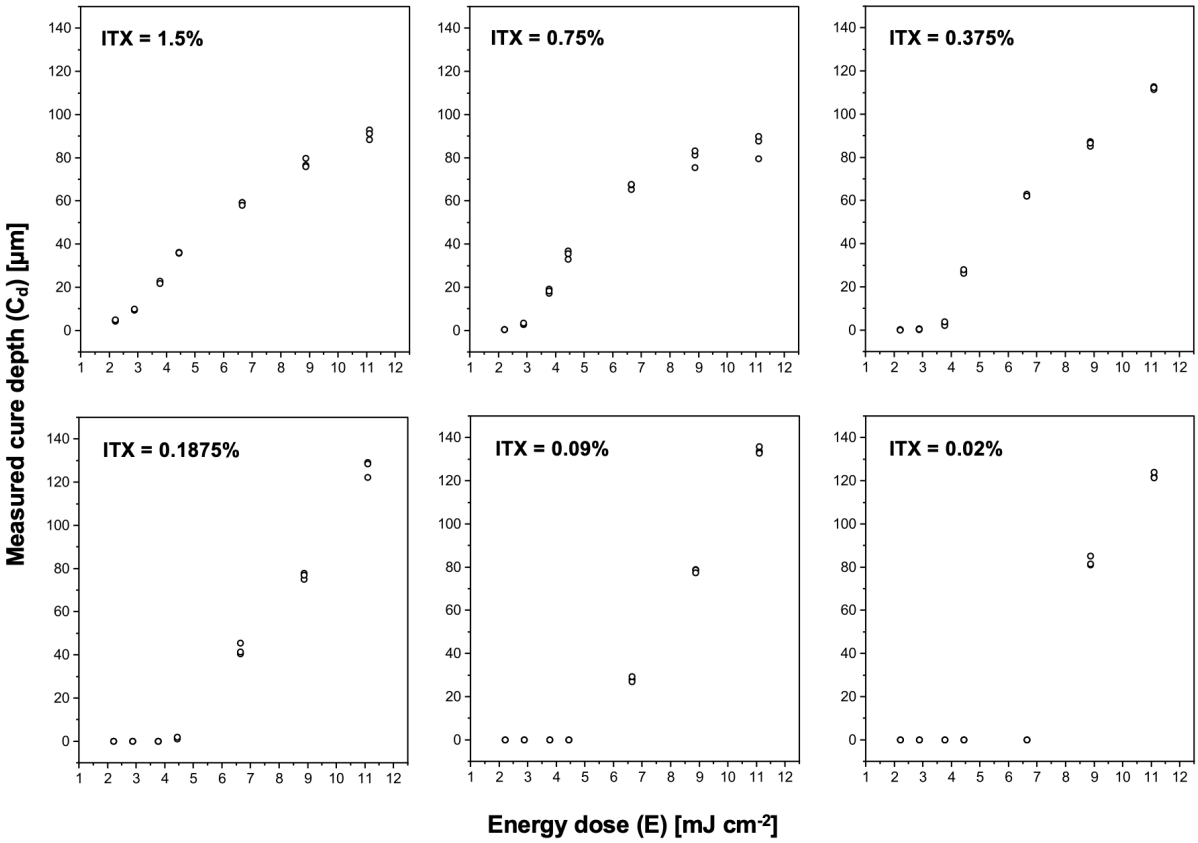

Figure S3. Cure depth as a function of the energy dose, for different concentrations of ITX to determine the penetration depth of light for PLInk. Data shows mean ± STD across three replicates and was acquired using the Elegoo Mars 3 Pro 3D printer.

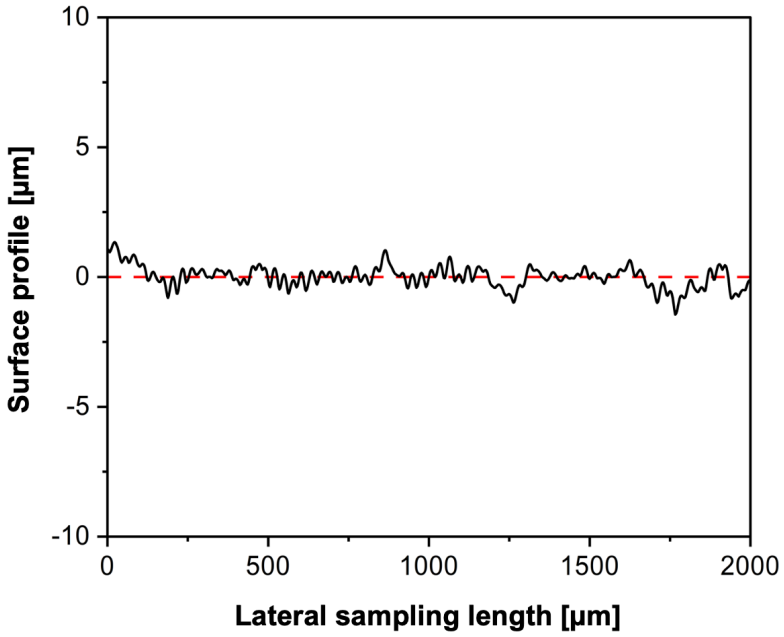

Figure S4. Surface roughness of 3D printed parts using PLInk. Surface topography given along a 12.5 µm line width using a stylus profilometer to calculate a mean surface roughness of 530 ± 110 nm across three replicates. Data was acquired using the Elegoo Mars 3 Pro 3D printer.

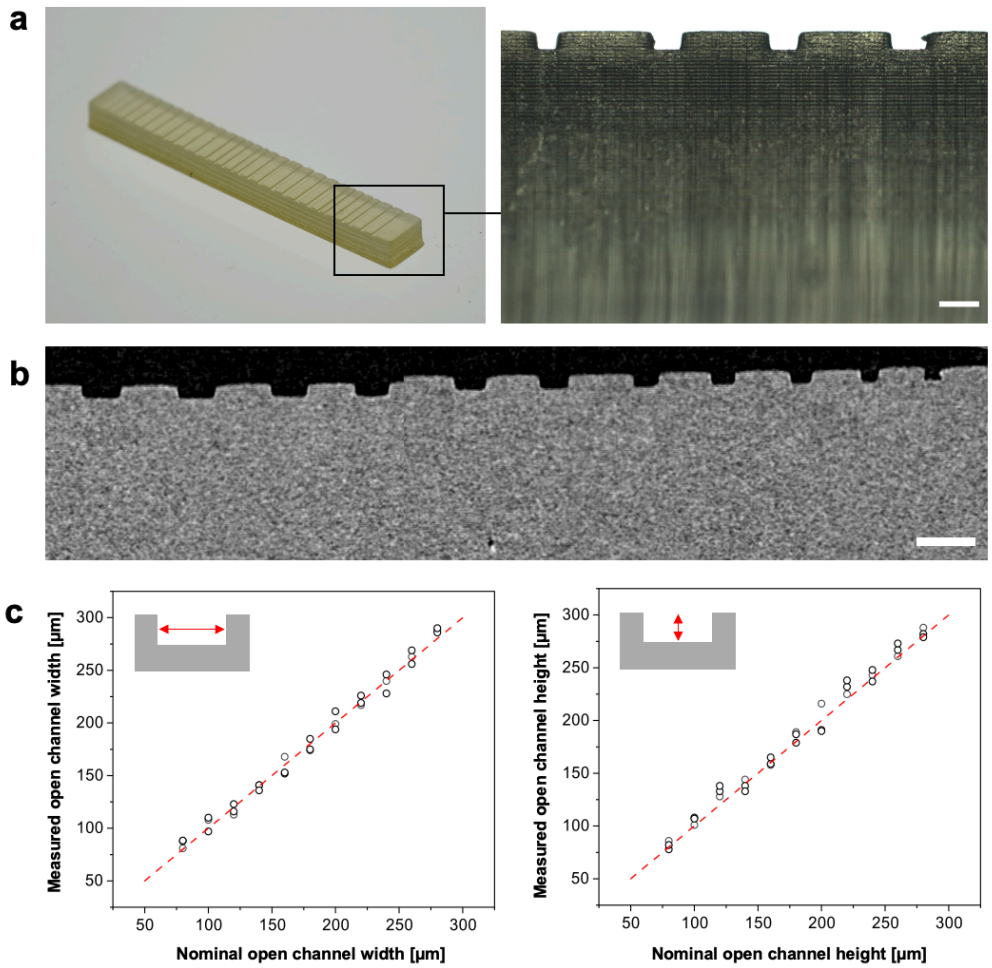

Figure S5. Open channel 3D printing. (a) Open channel calibrator device showing varying channel dimensions to assess the resolution, inset shows ~75 × 75 µm^2 open channel at the surface of the device. Scale bar = 200 µm. (b) µCT side view of the open channel calibrator device. Scale bar = 500 µm. (c) Dimensional accuracy between design file and printed channel widths and depths across three unique devices. Dashed line shows the case where the nominal value = measured value.

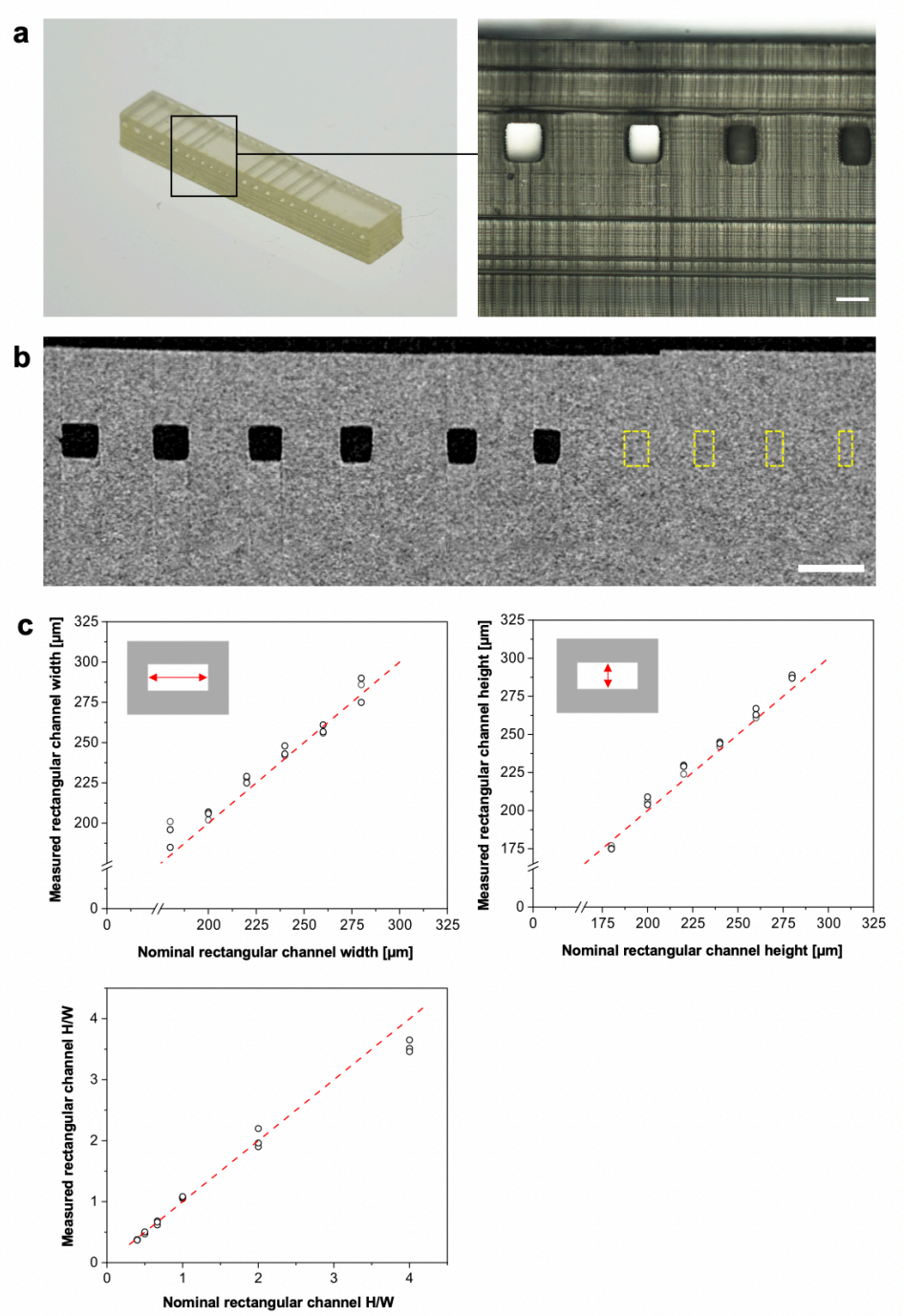

Figure S6. Rectangular channel 3D printing. (a) Rectangular channel calibrator device showing varying channel dimensions to assess the resolution, inset shows ~170 × 220 µm^2 rectangular channel embedded into the device. Scale bar = 200 µm. (b) µCT side view of the rectangular channel calibrator device showing clogged channels in yellow dashed outlines. Scale bar = 500 µm. (c) Dimensional accuracy between design file and printed channel widths and depths across three unique devices; aspect ratio dimensional accuracy is given as the height (H) divided by width (W) of rectangular microchannels. Dashed line shows the case where the nominal value = measured value.

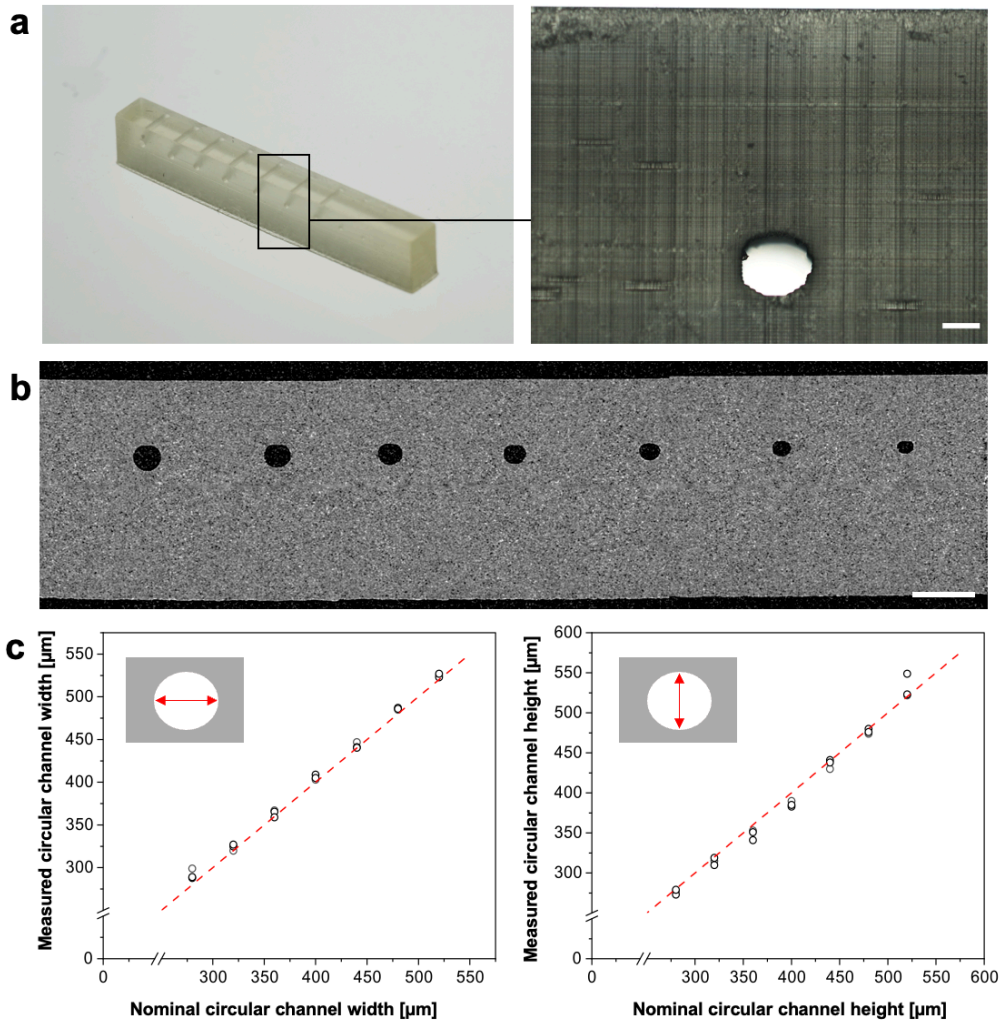

Figure S7. Circular channel 3D printing. (a) Circular channel calibrator device showing varying channel diameters to assess the resolution, inset shows a ~125 µm radius embedded channel. Scale bar = 200 µm. (b) µCT side view of circular channel calibrator device. Scale bar = 1 mm. (c) Dimensional accuracy between design file and printed channel widths and depths across three unique devices. Dashed line shows the case where the nominal value = measured value.

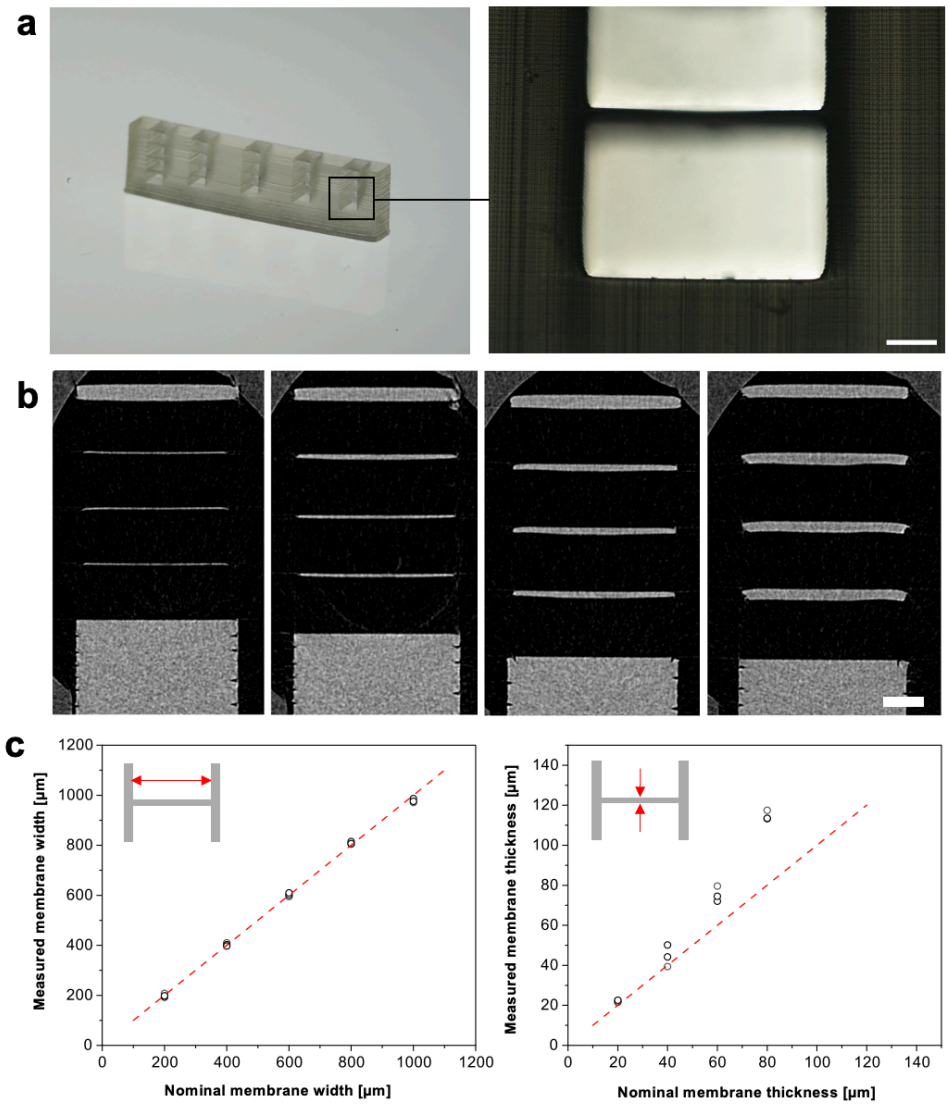

Figure S8. *In situ* membrane 3D printing. (a) Membrane calibrator device showing varying membrane thicknesses to assess the z-resolution, inset shows a 20 µm membrane. Scale bar = 200 µm. (b) µCT side views of 20, 40, 60, and 80 µm thick membranes. Scale bar = 500 µm. (c) Dimensional accuracy between design file and printed membrane widths and thickness across three unique devices. Dashed line shows the case where the nominal value = measured value.

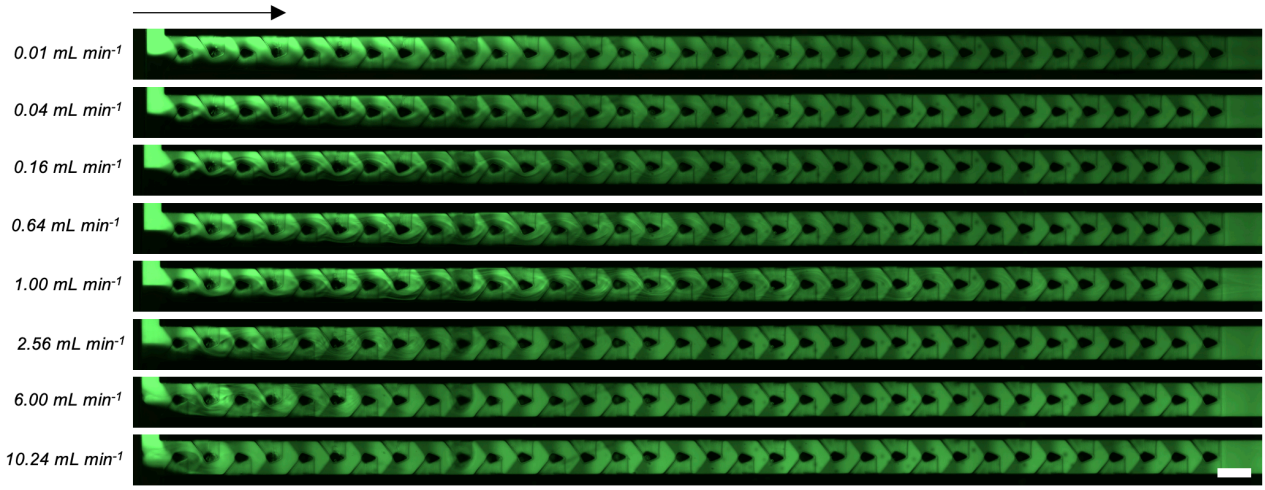

Figure S9. Fluorescent images of microfluidic mixing at different volumetric flow rates. Deionized water and 10 μM fluorescein solution were mixed over a range of flow rates from 0.01-10.24 mL min^{-1} via fluorescence microscopy along the length of the channel. Arrow shows the direction of flow. Scale bar = 1 mm.

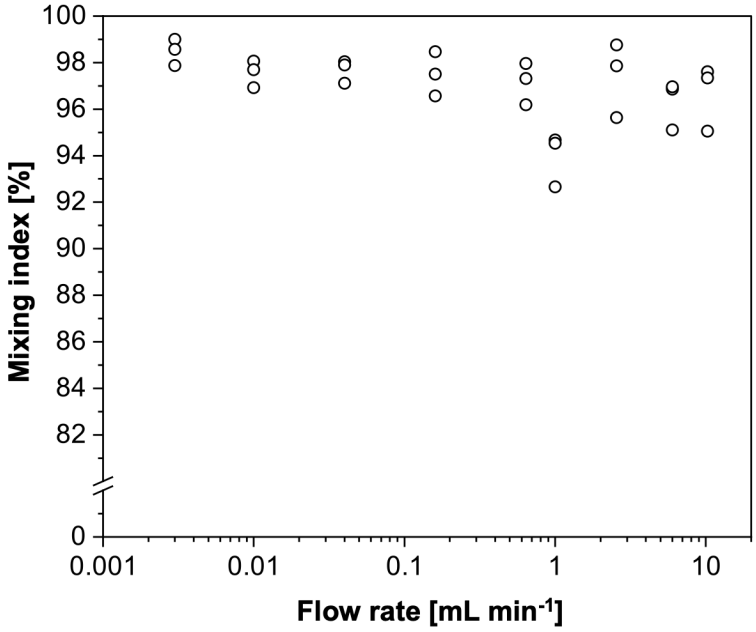

Figure S10. Mixing indices, shown for the mixing of 10 μM fluorescein and deionized water at different flow rates for three replicate micromixer devices.

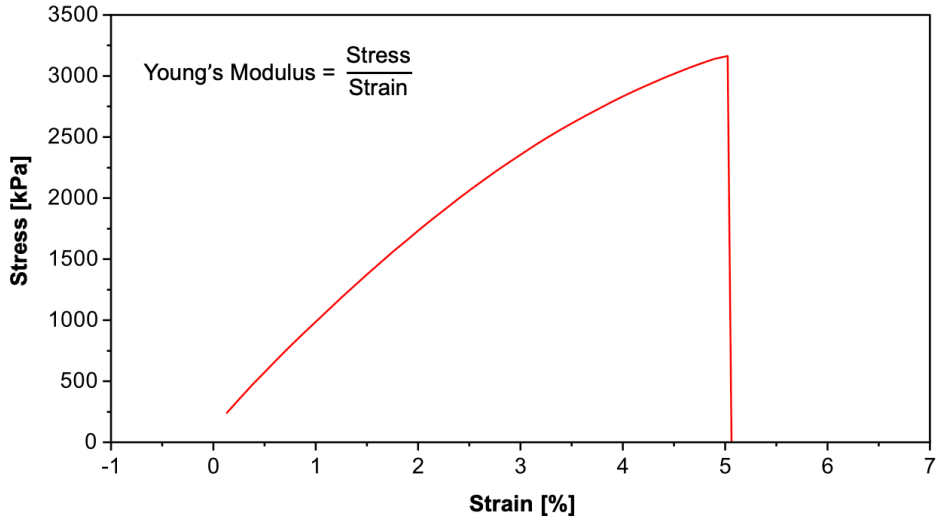

Figure S11. Tensile testing of 3D printed parts using PLInk. Application of a known load and observation of the measured extension gives a Young's modulus of 68 ± 3 MPa across three replicates.

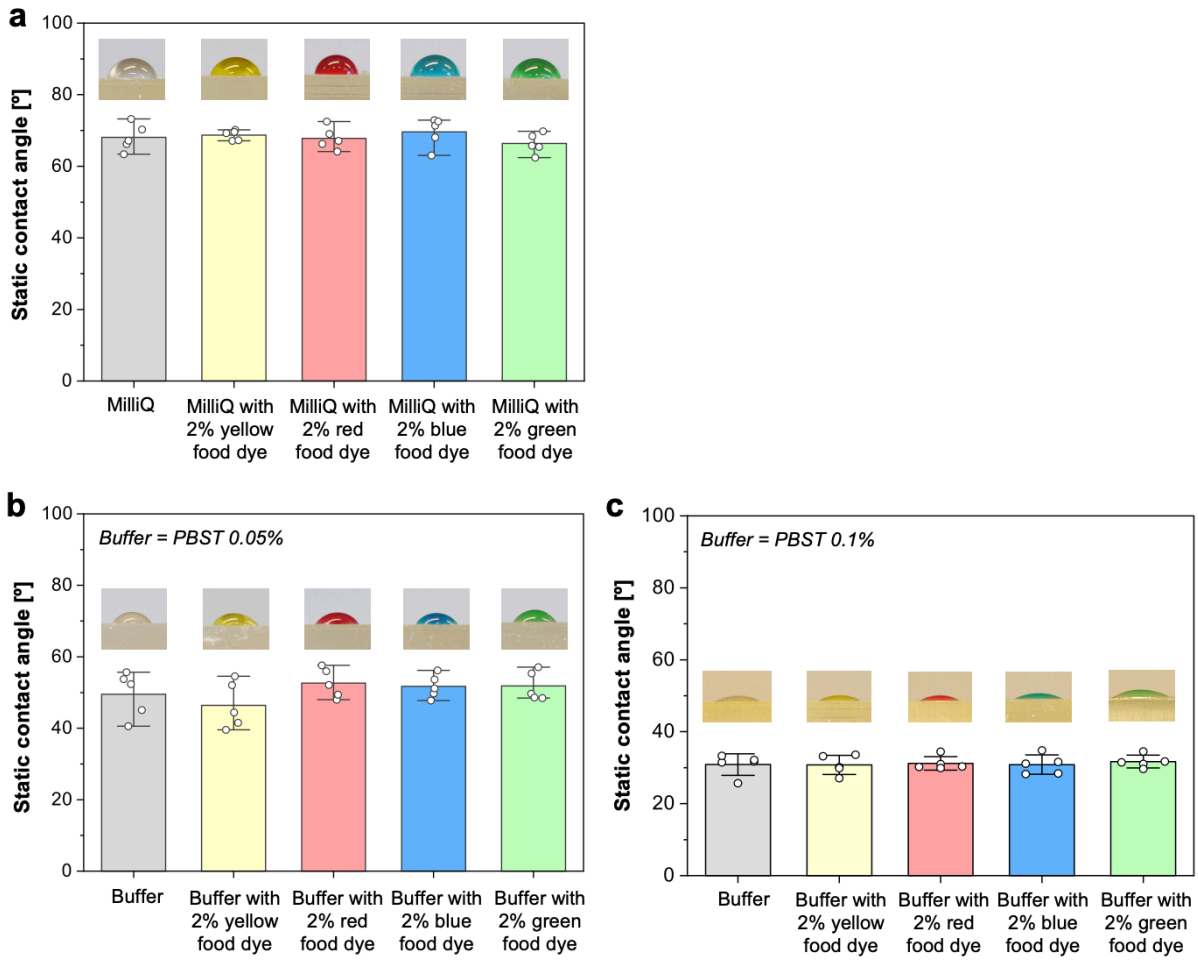

Figure S12. Contact angle. Contact angle of (a) water, (b) PBST 0.05%, and (c) PBST 0.1% ELISA buffer on 3D printed PLInk. Data shows mean ± STD across five replicates. Notably, this ink is inherently more hydrophilic than most commercial counterparts that we previously used for capillarics.[3, 4]

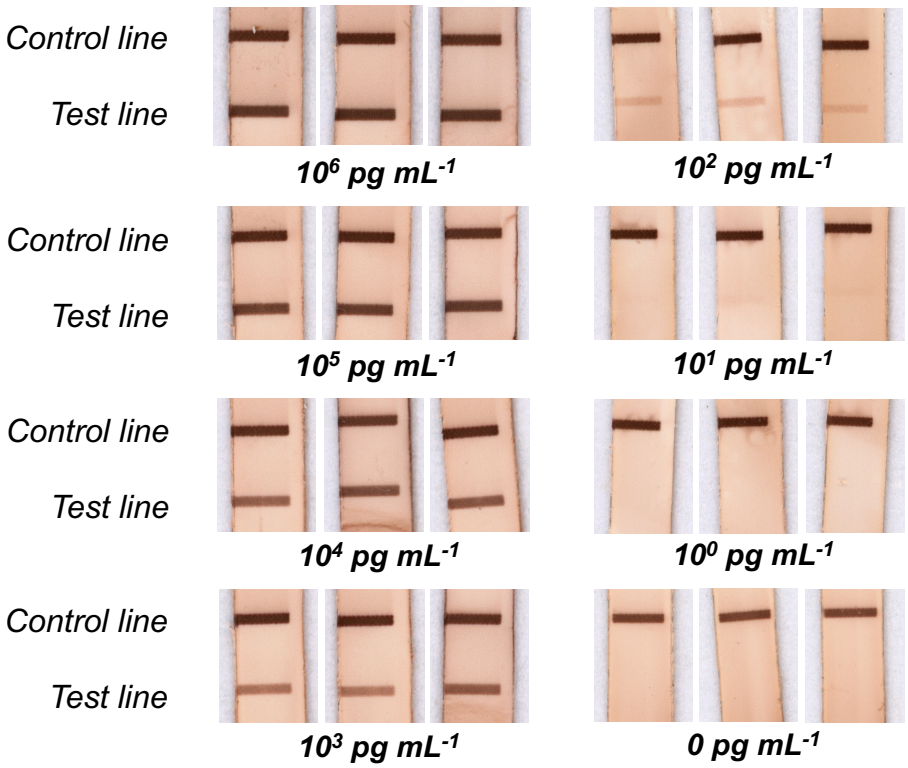

Figure S13. Nitrocellulose membranes from LCD 3D printed ELISA-chip for IFN-γ detection. Colorimetric readouts on a nitrocellulose membrane showing a control line and test line at various IFN-γ concentrations.

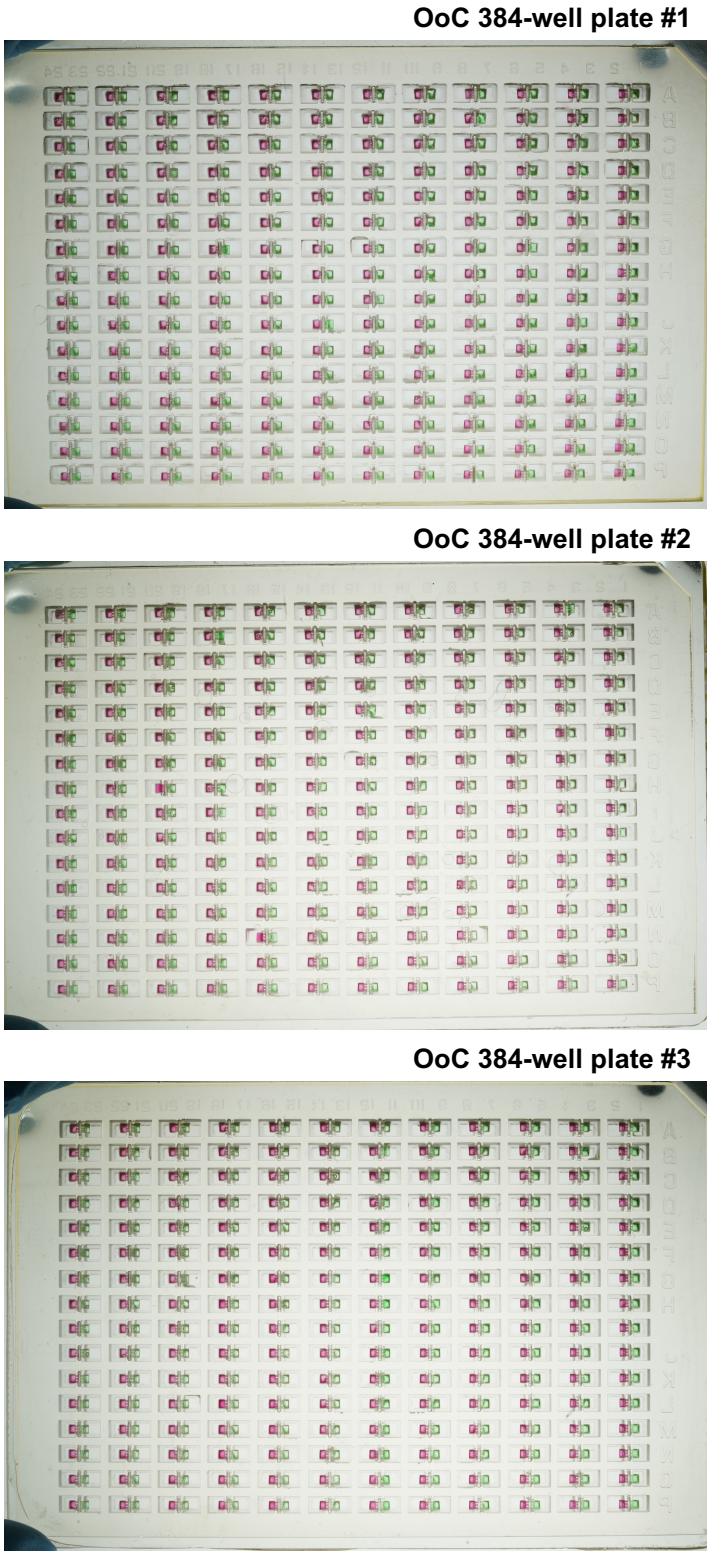

Figure S14. 384-well plate OoCs. Loading of red and green dyed gel solutions into the 384-well plate format OoC devices printed in 1.5 h using the Elegoo Saturn 3 Ultra with a nominal pixel size of 19 × 24 μm^2 and >58M pixels. Across three uniquely 3D printed well plates, we observe a 100% yield on fluidic performance of the embedded multi-layer stop valves.

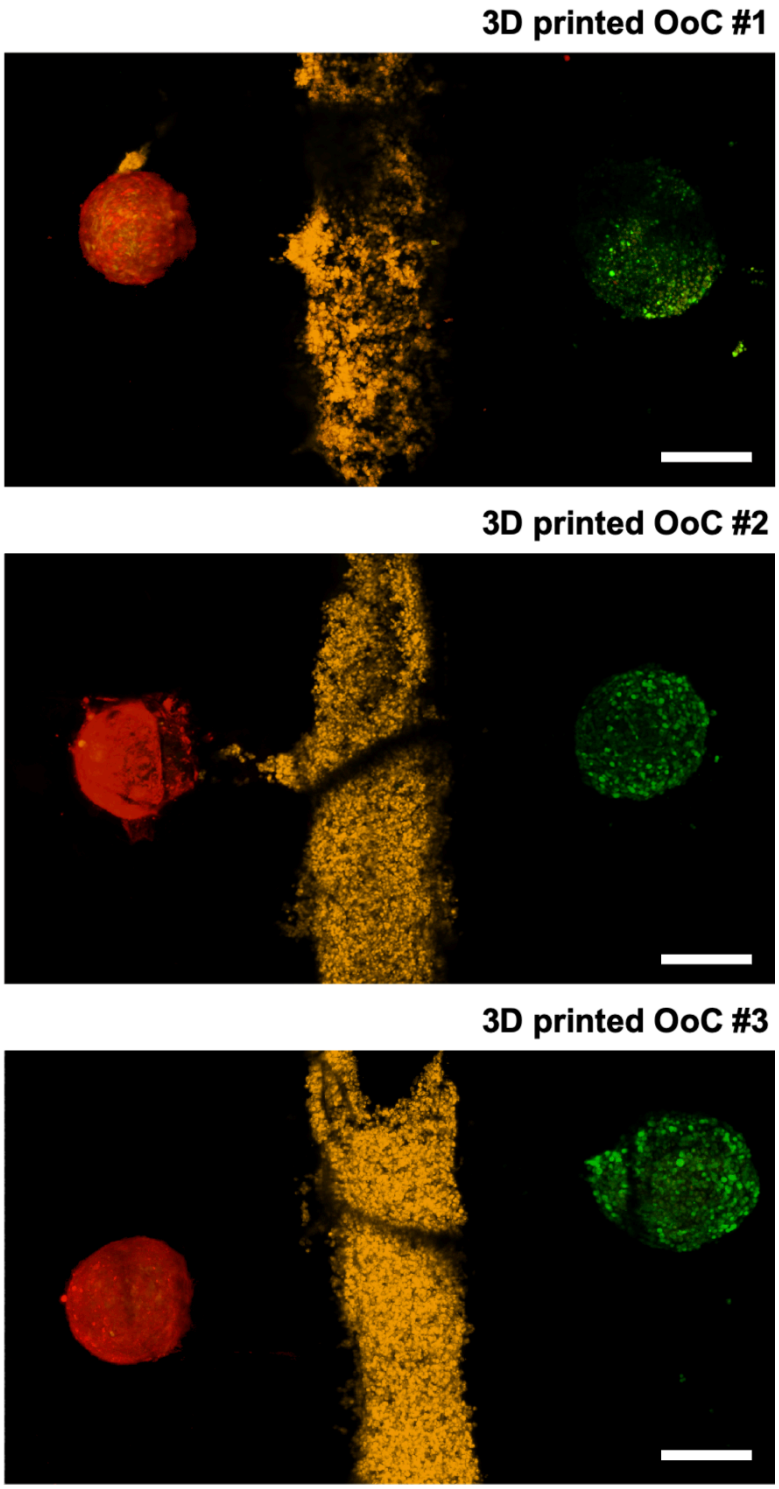

Figure S15. Cell seeding of OoC devices. Three individual OoC devices seeded with breast cancer spheroid (green), lung spheroid (red) and the middle chamber seeded with endothelial cells (orange) that form a vascular barrier.

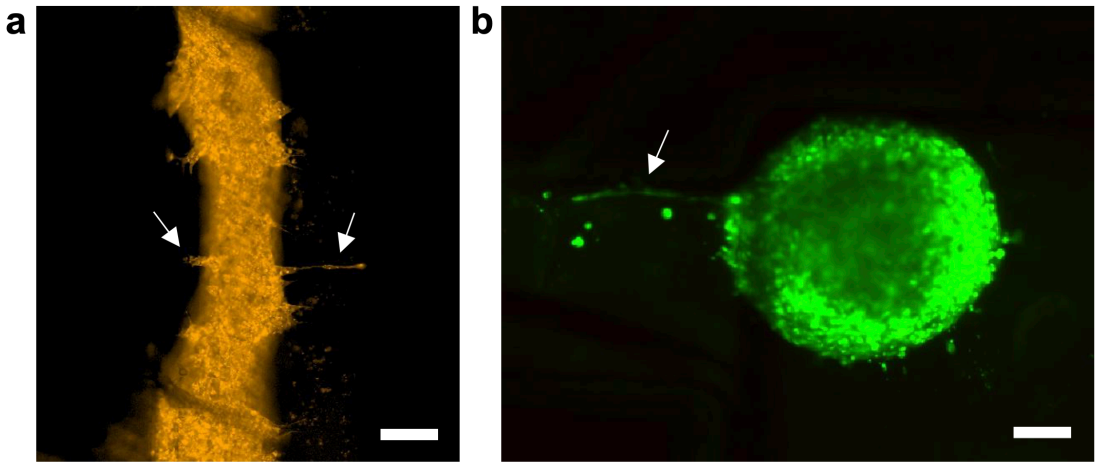

Figure S16. Cellular migration and reorganization after 5 days in the OoC device. (a) Endothelial cell tightening and sprouting of single cells towards the spheroid chambers. (b) Breast cancer spheroid showing initial cell migration towards the endothelial central chamber. Scale bars = 100 µm.

References:

1. Y.-S. Lee, N. Bhattacharjee and A. Folch, *Lab on a Chip*, 2018, **18**, 1207-1214.
2. W. Luo, M. Pla-Roca and D. Juncker, *Analytical Chemistry*, 2011, **83**, 5767-5774.
3. M. Yafia, O. Ymbern, A. O. Olanrewaju, A. Parandakh, A. Sohrabi Kashani, J. Renault, Z. Jin, G. Kim, A. Ng and D. Juncker, *Nature*, 2022, **605**, 464-469.
4. A. Parandakh, O. Ymbern, W. Jogia, J. Renault, A. Ng and D. Juncker, *Lab on a Chip*, 2023, **23**, 1547-1560.